Thermal, Electrical and Mechanical Response to a Quench in Nb_3Sn Superconducting Coils

P. Ferracin, S. Caspi, L. Chiesa, S.A. Gourlay, R.R. Hafalia, L. Imbasciati, A.F. Lietzke, G. Sabbi, and R.M. Scanlan

Abstract—During a quench, significant temperatures can arise as a magnet's stored energy is dissipated in the normal zone. Temperature gradients during this process give rise to localized strains within the coil. Reactive forces in the magnet structure balance the electromagnetic and thermal forces and maintain on equilibrium. In this paper we present a complete 3D finite element analysis of a racetrack coil. Specifically, the analysis focuses on thermal, electrical and mechanical conditions in a 10 T Nb_3Sn coil built and tested as part of LBNL's Subscale Magnet Program. The study attempts to simulate time history of the temperature and voltage rise during quench propagation. The transient thermal stress after the quench is then evaluated and discussed.

***Index Terms*—Superconducting magnets, quench propagation, thermal analysis, stress analysis.**

I. Introduction

WHEN a superconducting magnet quenches, the normal zone propagates and dissipates the stored magnet energy [1]. Avoiding conductor damage requires limiting the peak temperature during this process, and is a key reliability issue for superconducting magnets, in particular in particle accelerators.

The Superconducting Magnet Group at Lawrence Berkeley National Laboratory (LBNL) has recently investigated, in collaboration with Fermi National Accelerator Laboratory (FNAL), how much a Nb_3Sn coil heats up during a quench before permanent degradation is observed. A test was carried out on a subscale racetrack coil equipped with quench heater, temperature sensor, and voltage taps to analyze the buildup of temperature and resistive voltages in the windings [2], similar to studies performed on HERA [3], SSC [4], RHIC [5] and LHC [6] magnets. Moreover, for the last two years, LBNL has been extending the use of the commercial code ANSYS® from steady-state mechanical and magnetic analysis to transient thermal-electrical studies. In a previous paper [7], a "proof-of-principle" 3D finite element model aimed at simulating the quench propagation in a racetrack coil has been described, and the numerical results have been compared with analytical formulas.

In this work, the model geometry has been completed by including the entire subscale magnet structure in order to simulate the quench heater experiment. The predicted temperature and voltage rises have been compared with measurements. Furthermore, the analysis is extended to the mechanical response to a quench. The thermo-mechanical strain generated by a quench-induced temperature rise has been studied in previous works, both experimentally [8] and numerically [9], [10]. We describe here the results of a structural analysis where the temperature profile evaluated by the thermo-electrical model is transferred to a 3D mechanical model. The evolution of the coil stresses during the quench propagation are investigated and discussed.

II. Subscale Magnet Program

In 2001, LBNL implemented a sub-scale magnet program to test the performance of advanced magnet concepts under relatively realistic magnet conditions [11]. The cross-section of the subscale magnet is shown in Fig. 1: the outer diameter is 240 mm and the longitudinal length is 305 mm. The cable is composed of 20 (0.7 mm diameter) Nb_3Sn strands. The bare cable has a nominal cross-section of 7.94 mm × 1.28 mm, with a continuous 0.12-mm-thick woven sleeve of fiberglass insulation. A double-layer coil module is wound around a single iron pole (island) in a flat racetrack configuration and vacuum-impregnated with epoxy resin. Two of these modules are assembled in a common-coil configuration, and compressed on both sides by iron pads.

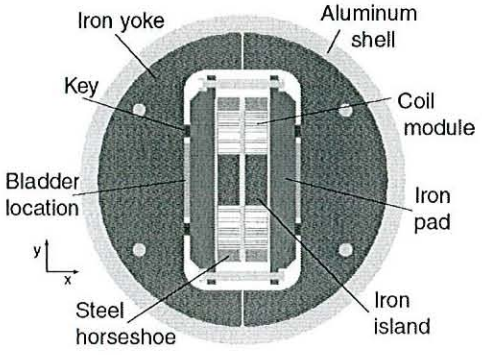

Fig. 1. LBNL subscale magnet cross-section.

Manuscript received October 20, 2003. This work was supported under contract DE-AD03-76SF00098 by the Director, Office of Energy Research, Office of High Energy Physics, U.S. Department of Energy.

S. Caspi, P. Ferracin, S. Gourlay, R. Hafalia, A. Lietzke, G. Sabbi, and R. Scanlan are with Lawrence Berkeley National Laboratory, Berkeley, CA 94720 (phone: 001 510 486 4630; fax: 001 510 486 5310; e-mail: pferracin@lbl.gov).

L. Chiesa is with MIT, Cambridge, MA.

L. Imbasciati was with Fermilab National Laboratory, Batavia, IL 60510.

The support structure consists of an iron yoke, an aluminum shell, and a set of four iron keys [12]. Two bladders generate the primary force needed to spread the yoke apart, tension the shell and pre-compress the coil-pack [13]. Once the structure is locked by the keys, the bladders are deflated and removed. During cool-down, the shell generates additional pre-load on the coil-pack, as a result of the different thermal contractions of aluminum and iron.

III. Finite Element Model

The finite element model of the subscale magnet is shown in Fig. 2. To simplify the analysis, the problem was split into two parts. The first part calculates the thermo-electric time-dependent quench response, while the second part computes the quasi-steady-state mechanical response to the developing temperature profile. The ANSYS model was created by importing a CAD solid model (ProE®), and assigning material properties, element types, boundary conditions and loads.

The thermo-electrical model includes the coils, the associated winding island, the confining horseshoe, and the pre-stressing pads. The yoke and shell were excluded. The volumes were "glued" in the model in a manner that permitted them to interact thermally on all surfaces. Each coil turn is electrically insulated by one layer of insulation, and modeled as a continuous series of straight and curved volumes, starting and ending with an open lead.

The mechanical model added the yoke and shell. The thermo-electric elements were replaced by similar structural elements and contact elements were added in the contact surfaces between components, allowing sliding or separation. The meshes of both models are identical, to facilitate the transfer of the temperature profiles to the mechanical model.

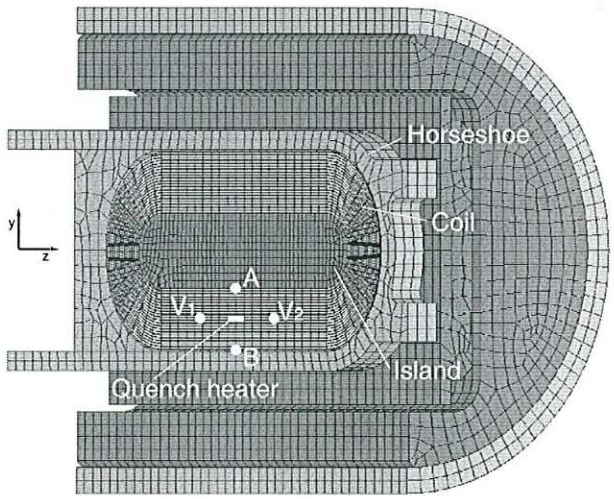

Fig. 2. Finite element model of the LBNL subscale magnet.

IV. Thermo-Electric Analysis: Quench Propagation

This section presents the experimental conditions of the quench-heater test, and the associated assumptions of the thermo-electrical model. The numerical computations and the experimental measurements are compared and discussed.

A. Experimental conditions

Spot-heater experiments began after the magnet reached 8757 A at 4.3 K, approximately 1 % above the computed short sample current. These experiments involved initiating quenches at various currents by pulsing a spot heater. The spot heater (8 mm × 15 mm) was sandwiched between two turns, located near the maximum field point of the coil, close to the center of the innermost layer (see Fig. 2). The power supply shut-off delay was systematically increased from 40 ms to 3500 ms after the quench detection. Nine heater-induced quenches were studied with an initial current of 3000 A.

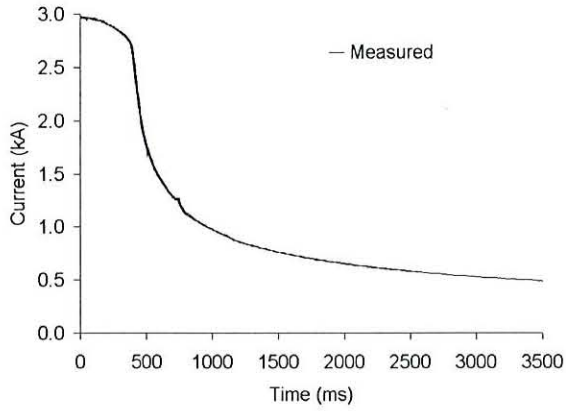

Fig. 3. Current decay during a heater-induced quench (measurements).

The combined effect of the coil's resistance development and the 61 V voltage limit of the power supply resulted in the magnet current history shown in Fig. 3. The current was nearly constant for 400 ms, until the power supply limit was reached, after which a rapid decay for the next 100 ms was followed by a slower decrease to 500 A at 3500 ms. Two voltage taps (V1 and V2 in Fig. 2) measured the voltage of a 90 mm long conductor segment, in which the quench heater was located. The total voltage of the coil was also recorded. The hot spot temperature was determined from the segment's resistivity, which was calibrated against temperature during the slow magnet warm-up.

B. Thermo-electrical model

The model uses 8-node thermal-electrical elements (SOLID69) for the cable and 8-node thermal elements (SOLID70) for the insulation and the support structure. The simulations were based on the following assumptions: 1) the experimentally measured current (Fig. 3) was imposed as a function of time, 2) all field-dependent material properties were evaluated at 4 T, corresponding to the peak field at the quench initiation location, with a current of 3000 A, 3) the cable electrical resistivity in the superconducting state was assumed to be very small, but finite (1.0×10^{-13} Ohm·m), 4) the resistivity transition from the superconducting state to the normal state varied linearly over a temperature range of 0.1 K starting at T_{cs} (corresponding to the current sharing temperature), 5) a quench was initiated by applying a power of 6.4 W to the heater, 6) the measured electrical resistivity, from

4.3 K to 330 K, was used as the resisitivity of the conductor, 7) the cable thermal conductivity was assumed to be that of pure copper, weighted according to its measured fraction of the entire cross-section, 8) the specific heat was computed from an average of the specific heat of copper, Nb_3Sn and epoxy, 9) the insulation was assumed to have properties identical to those of G10 in the direction perpendicular to the fibers, 10) all the temperature-dependent thermal and electrical material properties were taken from [14], 11) adiabatic boundary conditions were assumed.

C. *Results*

In Fig. 4, the resistive voltage across the 90 mm long segment is plotted, from the quench initiation time (assumed to be at 0 ms) up to 3.5 s. Excellent agreement was observed between measured and computed results. The rapid voltage rise during the first 20 ms is mostly due to quench propagation. Once the segment is completely normal, a more slower voltage rise results from temperature increase. The segment voltage reaches its maximum value of 0.8 V at 380 ms followed by a rapid decay to 0.4 V as the current decreases sharply.

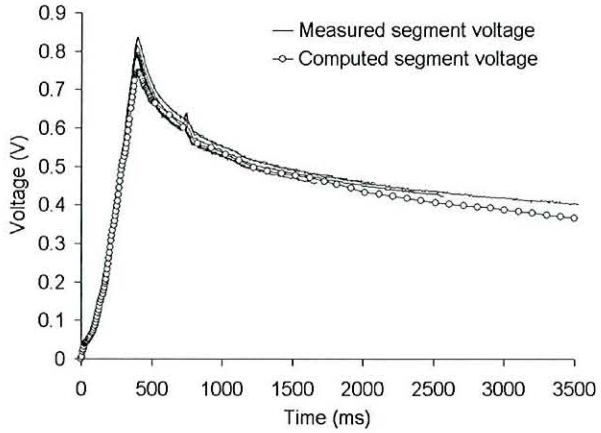

Fig. 4. Measured (solid lines) and computed (round markers) transient voltage in a 90 mm conductor segment (V_2-V_1 in Fig. 2) surrounding the hot spot during a quench.

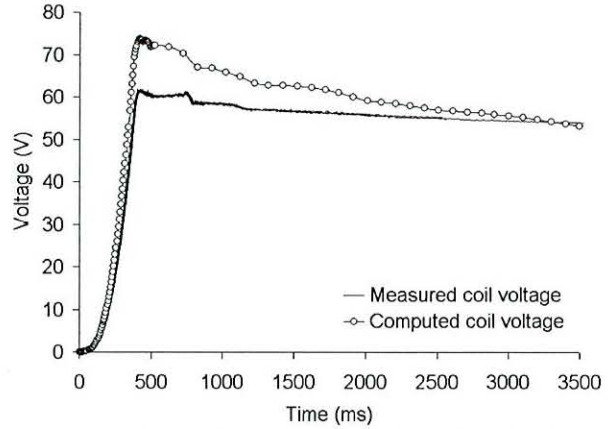

Fig. 5. Measured (solid lines) and computed (round markers) transient voltage of the two-layer coil during a quench.

The resistive voltage of the entire coil (both layers) follows a similar pattern (Fig. 5). The computed voltage reaches a maximum of 74 V at 380 ms, compared with 61 V measured. According to the computations, the normal zone, initiated in the inner layer, conducts heat into the outer layer, which starts quenching after 86 ms. Despite the 86 ms delay in quench initiation, pre-heating increases the quench propagation velocity of the outer layer, so that both layers happen to become completely normal at the same time of 321 ms. Once the peak voltage is reached, the increase in electrical resistivity due to the temperature is compensated by the decrease of the supplied current, thus maintaining an almost constant total voltage across the coil.

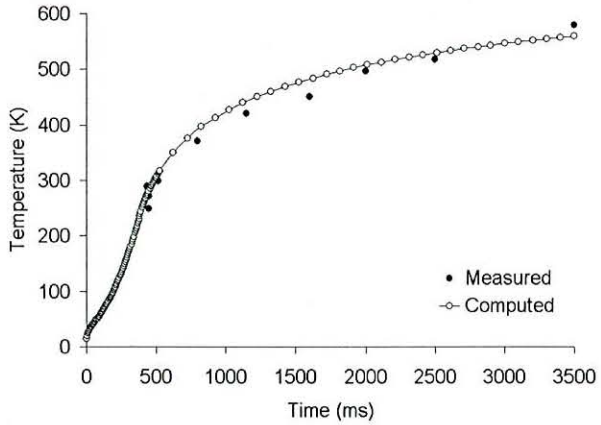

Fig. 6. Measured (black markers) and computed (white markers) hot spot temperature.

In Fig. 6, the computed hot spot temperature response is in very good agreement with the measurements. It is important to notice that, despite the high temperature reached after 3.5 s (590 K), only a slight degradation from "short-sample" coil performance was observed [2].

V. Mechanical Analysis: Response to a Quench

The mechanical model allows evaluating the transient stress distribution within the coil during quench propagation. In this section the mechanical model's main features and assumptions are described. Calculation results in the region near the peak temperature, where the quench heater is located, are presented and discussed.

A. *Mechanical model*

The model uses 8-nodes (SOLID45) and 20-nodes (SOLID95) brick elements for the coil and the mechanical components respectively. The simulation is based on the following assumptions: 1) the turns and the insulation are handled similarly to the thermo-electric model and assigned the elastic modulus of epoxy-impregnated Nb_3Sn composites, 2) a temperature dependent thermal contraction of the coil between 4.3 K and 300 K has been implemented [14], 3) the temperature profile of the coil computed during quench propagation is read at each time step as a thermal load, while the temperatures of the support components are assumed to remain at 4.3 K, 4) the Lorentz forces at 3000 A are neglected, 5) contact elements (TARGE170 and CONTA174) are defined between all the surfaces permitting sliding and separation of components.

B. Results

Transverse (turn-to-turn) profiles of the conductor stress components were computed over the 30 mm winding thickness of the coil (from point A to point B in Fig. 2) during the first 480 ms, while the temperature of the quench initiation site rose from 4.3 K to 300 K. The evolutions of these profiles are depicted in Fig. 7-9, where each curve represents a given stress component at the indicated peak temperature and time after the quench initiation. Curve *a* (the horizontal line at 0 ms) shows the stress achieved after the cool-down, when the coil is in mild longitudinal (z) tension (40 MPa) due to its higher thermal contraction relative to the iron island.

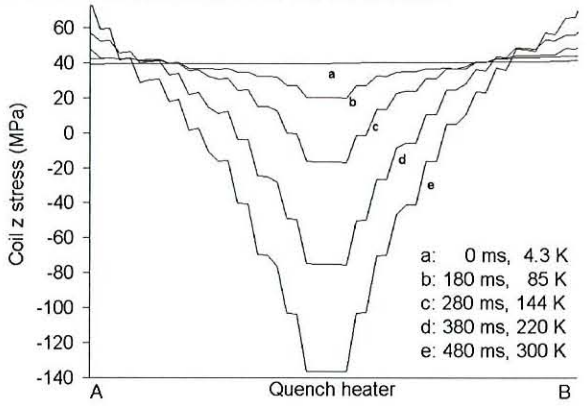

Fig. 7. Longitudinal (z) stress computed in the coil during a quench as a function of position across the coil (path A – B, Fig. 2).

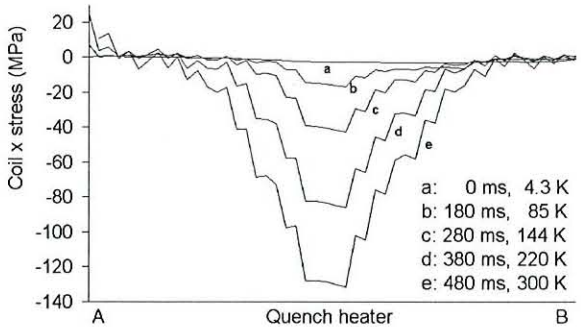

Fig. 8. Horizontal (x) stress computed in the coil during a quench as a function of position across the coil (path A – B, Fig. 2).

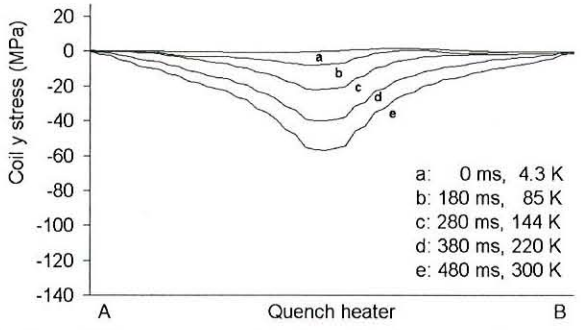

Fig. 9. Vertical (y) stress computed in the coil during a quench as a function of the position across the coil (path A – B, Fig. 2).

After the quench is initiated, the hotter regions attempt to expand and push against the colder surroundings. In particular, this expansion is reacted by the tension in the cold outer shell, the cold horseshoe and the relatively cold late-quenching turns. The hot spot experiences compression in every direction after the quench. The maximum longitudinal compression after 480 ms (curve *e*, Fig. 7) is about 140 MPa. A similar value is calculated for the x direction (Fig. 8), which is constrained by the pads. In the vertical direction (Fig. 9), the peak compression is much lower (55 MPa at 480 ms), since the coil is relatively free to expand. Stresses calculated for temperatures above 300 K are not reported because authoritative mechanical properties have not yet been completely established in this temperature range. Simplistic extrapolations of the 300 K dependences yielded high compressive conductor stresses (about 300 MPa) at the peak temperature (590 K).

VI. Conclusions

The time-dependent thermal, electrical, and mechanical quench response of a Nb_3Sn coil was studied. A finite element model was used to calculate racetrack-type coil temperatures and voltages during a heater-induced quench. Calculations predicted voltages and peak temperatures that agreed well with experimental measurements. The inferred temperature distributions were inputted into a mechanical model to compute the associated thermo-mechanical stress. The analysis predicted, 480 ms after a 3000 A quench, a peak compressive conductor stress of 140 MPa.

References

[1] M.N. Wilson, *Superconducting Magnets*, Clarendon Press, Oxford, 1983, ch. 9.

[2] L. Imbasciati *et al.*, "Study of the effects of high temperature during quenches on the performance of a small Nb_3Sn racetrack magnet", presented at the 6th European Conference on Applied Superconductivity, Sorrento, Italy, September 14-18, 2003.

[3] D. Bonmann *et al.*, "Investigation on heater induced quenches in a superconducting test dipole for the HERA proton accelerator", DESY Report HERA 87-13, 1987.

[4] A. Devred *et al.*, "Investigation of heater induced quenches in a full-length SSC R&D dipole", in *Proc. 11th International Conference on Magnet Technology*, Tsukuba, 1989, Vol. 1, pp. 91-95.

[5] J. Muratore *et al.*, "Quench propagation study for full-length RHIC dipole magnets", *IEEE Trans. Magn.*, vol. 30, no. 4, July 1994,pp. 1726.

[6] L. Coull *et al.*, "Quench propagation tests on the LHC superconducting magnet string", *Proc. 5th European Conference on Particle Accelerators*, Sitges, 1996, pp. 2249-2251.

[7] S. Caspi *et al.*, "Calculating quench propagation with ANSYS®", *IEEE Trans. Appl. Superconduct.*, vol. 13, no. 2, June 2003, pp. 1714-1717.

[8] L. Imbasciati, *et al.*, "Effect of thermo-mechanical stress during quench on Nb_3Sn cable performance", *IEEE Trans. Appl. Superconduct.*, vol. 13, no. 2, June 2003, pp. 1718-1721.

[9] D. Perini, and F. Rodriguez-Mateos, "Calculation of the thermo-structural transient in LHC dipole at quench", *IEEE Trans. Magnetics*, vol. 28, no. 1, January 1992, pp. 370-373.

[10] R. Yamada *et al.*, "2-D/3-D quench simulation using ANSYS for epoxy impregnated Nb_3Sn high field magnets", *IEEE Trans. Appl. Superconduct.*, vol. 13, no. 2, June 2003, pp. 1696-1699.

[11] R.R. Hafalia *et al.*, "An approach for faster high field magnet technology development", *IEEE Trans. Appl. Superconduct.*, vol. 13, no. 2, June 2003, pp. 1258-1261.

[12] R.R. Hafalia *et al.*, "A new support structure for high field magnet", *IEEE Trans. Appl. Superconduct.*, vol. 12, no. 1, March 02, pp. 47-50.

[13] S. Caspi *et al.*, "The use of pressurized bladders for stress control of superconducting magnets", *IEEE Trans. Appl. Superconduct.*, vol. 11, no. 1, March 2001, pp. 2272-2275.

[14] CRYOCOMP, CryoData Inc., PO Box 173, Colorado 80027, USA.